

X-ray diffraction diagnostics of laser structures

K. M. Pavlov, V. I. Punegov, and N. N. Faleev*

Syktvykar State University, 167001 Syktvykar, Russia

(Submitted 11 October 1994)

Zh. Éksp. Teor. Fiz. **107**, 1967–1982 (June 1995)

By means of high-resolution x-ray diffractometry techniques (two-crystal diffractometry and a three-crystal scheme in the $(\vartheta-2\vartheta)$ scanning regime), the inverse problem of x-ray diffraction in a laser heterostructure with quantum-sized active region has for the first time been formulated and solved numerically. Profiles of the elastic deformation distribution, the static Debye–Waller factor, and the dimensions of the microdefects have been obtained as functions of thickness in a multilayer system, and a correlation has been established between the crystalline perfection of laser structures and the degradation characteristics of laser diodes. © 1995 American Institute of Physics.

I. INTRODUCTION

The vigorous development of micro-electronics and, associated with it, the creation of new composite materials, have been accompanied by the perfection of old methods, and the appearance of new ones for nondestructive testing of material structures, based on the scattering of x-rays in a condensed medium.^{1–4} Among the relatively new objects of study, one can mention multilayer systems with quantum wells based on GaAs/GaAlAs and other $A_{III}B_V$ compounds.⁵

Methods of high-resolution x-ray diffractometry are widely used to investigate heterostructures.^{6–10} These methods allow one to determine the mismatch parameters, thicknesses of the epitaxial layers and interfaces, and profiles of the deformation distribution (concentration composition) in heterostructures, and also to investigate the crystalline perfection of multilayer structures as a whole. This parameter is very important since the perfection of a multilayer system is an objective criterion of the epitaxial technology and allows one to produce a catalog of optimal regimes of epitaxial growth. The defectiveness of the structure strongly influences the electrophysical parameters of devices—the magnitude of the threshold current, the breakdown voltage and leakage currents, the noise level and the rate of degradation. Structural perfection is especially important for devices working at high current densities and optical radiation densities since these factors substantially influence the mobility of the defects and their structural transformations.

Present-day methods of high-resolution x-ray diffractometry—these include interference methods^{6–8} and differential^{9,10}—possess high sensitivity and spatial resolution. For some types of heterostructures the resolution of these methods is comparable with the resolution of an electron microscope, but in this case they have a much wider range of applicability. All this allows one to determine the structural parameters of epitaxial layers, even quantum-sized, with high accuracy, and to examine in detail the mechanisms of epitaxial growth and defect formation in any type of heterostructure.

Along with the appearance of the new experimental techniques, the statistical dynamic theory of x-ray diffraction in multilayer heterostructures with randomly distributed microdefects has undergone further development.^{11–15} An

analysis of the results so obtained and numerical modeling of the diffractive reflection curves have demonstrated the influence of the angular distribution of the diffusely scattered intensity on the formation of the entire diffractive reflection curve for reflection from various multilayer systems. It may be supposed that the integrated application of new experimental and theoretical methods will make it possible to obtain more accurate and complete data on the profile of the deformation distribution in multilayer heterostructures, to determine the type of crystalline defects and the profile of their distribution with depth, to determine the interrelationship between the conditions of epitaxial growth and the structural parameters, and to determine their influence on the electrophysical characteristics of devices.

The structural parameters of a multilayer crystalline system are often found by the simple scheme of solving the direct diffraction problem.^{16,17} However, such a fitting procedure more often than not does not give satisfactory agreement between the theoretical and experimental results for complex multilayer systems such as laser heterostructures. Significant difficulties arise due to the large number of fitting parameters. Choosing simple models of the structure does not always lead to the desired outcome. Therefore it is necessary to turn to the more laborious process of solving the inverse problem.^{18,19} Such problems are solved by numerical methods, e.g., by minimizing the error functional.²⁰ It is necessary at the same time to confront the problem of nonuniqueness of the solution.^{18,21} In the case under consideration this problem is gotten around with the help of additional a priori information about the investigated structure.

So far, calculational x-ray diffraction diagnosis of multilayer systems has been carried out, as a rule, without account of diffuse scattering by defects. Taking into consideration the fact that structural defects strongly influence the formation of the entire two-crystal diffractive reflection curve, in the present paper we have undertaken an unprecedented effort to solve the inverse problem of dynamic x-ray diffraction in a laser structure by simultaneously using the results of two- and three-crystal diffractometry. Such an approach takes into account the behavior of the angular distribution of the coherent and diffuse components of the scattered intensity and allow one to obtain information not only about the profile of the concentration composition of the het-

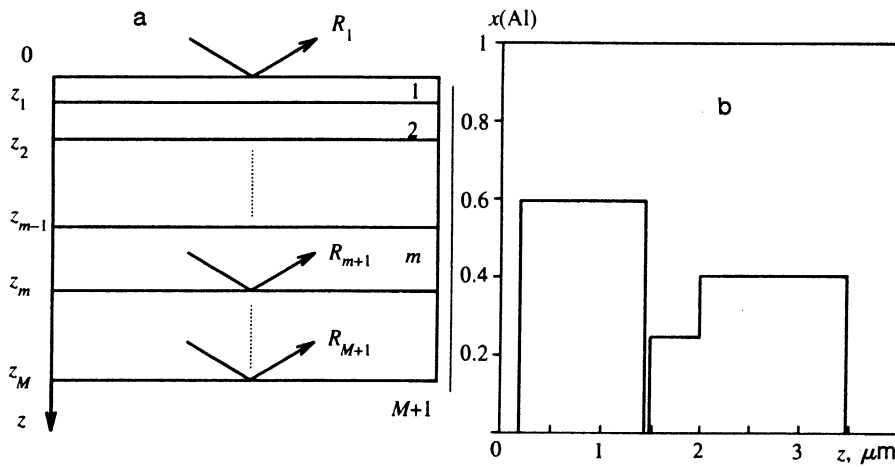


FIG. 1. Diffraction scheme in a multilayer system (a) and design profile of the chemical composition of the laser heterostructure with a quantum-sized well (b).

eroheterostructure, but also about the concentration, type, and dimensions of the randomly distributed defects.

2. ALGORITHMS FOR SOLVING THE INVERSE PROBLEM

To solve the inverse diffraction problem successfully, it is first of all necessary to formulate the algorithm of the calculational procedure. In the case under consideration it should be based on the following two main premises: first, the problem of diffraction in a multilayer structure requires the use of recurrence relations;^{14,19,22} second, the influence of microdefects on the formation of the entire two-crystal rocking curve can be accounted for within the framework of the statistical dynamic theory of diffraction.¹¹⁻¹⁵

To develop an algorithm for calculational diagnosis of the parameters of a laser heterostructure from x-ray diffraction data, we will consider the following model of a multilayer system (Fig. 1a): the crystalline structure consists of M layers of different thickness, each of which, for example, the m th one, is characterized by its own interplanar distance d_m , static Debye-Waller factor E_m , and mean defect dimension r_m . This entire multilayer system lies on a thick substrate (modeled as a semi-infinite crystal), referred to as the $(M+1)$ th layer. Strictly speaking inside the volume of any given layer and on its hetero-boundaries defects are formed, different in provenance and spatial structure. Since an analytical search for a common correlation function of the various randomly distributed defects is at present for all intents an unsolvable problem, it is necessary to use either an artificially constructed simple model characterizing the mean size of the defects (e.g., of Gaussian type¹²) or to refine the predominant form of the defects with the help of one of the available techniques^{4,23} and then employ the model corresponding to these defects in the calculation (for point defects or clusters, a "Coulomb" model²³).

In the case of symmetric Bragg diffraction the amplitudes of the transmitted $E_{0,m}^c$ and diffracted $E_{g,m}^c$ coherent waves in the layer with index m as functions of the angular deviation $\Delta\vartheta = \vartheta - \vartheta_0$ and the coordinate z can be represented in the following form:

$$E_{0,m}^c(z, \Delta\vartheta) = A_1^{(m)} \exp(i\zeta_1^{(m)} z) + A_2^{(m)} \exp(i\zeta_2^{(m)} z),$$

$$E_{g,m}^c(z, \Delta\vartheta) = k_1^{(m)} A_1^{(m)} \exp(i\zeta_1^{(m)} z) + k_2^{(m)} A_2^{(m)} \exp(i\zeta_2^{(m)} z), \quad (1)$$

where the coefficients $A_{1,2}^{(m)}$ are found from the boundary conditions. The remaining coefficients in solution (1), in conventional notation,²⁴ have the form

$$k_{1,2}^{(m)} = \frac{\zeta_{1,2}^{(m)} - \sigma_0^{(m)} - i\rho}{\sigma_{-g}^{(m)} E^{(m)}}, \quad \zeta_{1,2}^{(m)} = \frac{-\eta^{(m)} \pm \zeta^{(m)}}{2},$$

$$\zeta^{(m)} = \sqrt{(\eta_d^{(m)})^2 - 4\sigma_g \sigma_{-g} (E^{(m)})^2}, \quad \eta_d^{(m)} = \eta^{(m)} + 2i\rho^{(m)},$$

$$\eta^{(m)} = \frac{\kappa}{\gamma_0} [\chi_0^{(m)} + (\Delta\vartheta + \Delta\vartheta_m) \sin 2\vartheta_0],$$

$$\rho^{(m)} = \sigma_g^{(m)} \sigma_{-g}^{(m)} [1 - (E^{(m)})^2] \tau^{(m)},$$

$$\Delta\vartheta_m = \frac{d^{(m)} - d}{d} \operatorname{tg} \vartheta_0,$$

$$\sigma_0^{(m)} = \frac{\pi\chi_0^{(m)}}{\lambda_0\gamma}, \quad \sigma_{g,-g}^{(m)} = \frac{\pi\chi_{g,-g}^{(m)} C}{\lambda_0\gamma}, \quad \gamma_0 = \sin \vartheta_0,$$

$$\kappa = \frac{2\pi}{\lambda}, \quad C = \begin{cases} 1, & \sigma\text{-polarization,} \\ \cos 2\vartheta_0, & \pi\text{-polarization,} \end{cases}$$

ϑ_0 is the Bragg angle, λ is the wavelength, and $\chi_{0,g,-g}$ are the Fourier components of the polarizability.

The parameter $\rho^{(m)}$ describes the diffuse absorption of the coherently scattered waves and is determined by the static Debye-Waller factor $E^{(m)} = \langle \Phi \rangle$ and the correlation length $\tau^{(m)}$. Here $\Phi = \exp(i\mathbf{g}\delta\mathbf{u})$ is the lattice phase factor, where \mathbf{g} is the diffraction vector, and $\langle \dots \rangle$ denotes averaging. In turn, the correlation length depends on the correlation function

$$g(\xi) = (1 - E^2)^{-1} \{ \langle \exp(-i\mathbf{g}[\delta\mathbf{u}(\xi) - \delta\mathbf{u}(0)]) \rangle - E^2 \}$$

where $\delta\mathbf{u}(\xi)$ are the random atomic displacements caused by the randomly distributed effects.

An expression (1) for the amplitude reflection coefficient (ARC) for reflection from the last $M-m$ layers follows immediately from the solution, in other words, the amplitude of the reflection at the m th heteroboundary and the $(m+1)$ th layer:

$$R_{m+1} = \frac{E_g^c(z_m)}{E_0^c(z_m)} = \frac{k_1^{(m)} A_1^{(m)} \exp(i \zeta_1^{(m)} z_m) + k_2^{(m)} A_2^{(m)} \exp(i \zeta_2^{(m)} z_m)}{A_1^{(m)} \exp(i \zeta_1^{(m)} z_m) + A_2^{(m)} \exp(i \zeta_2^{(m)} z_m)}.$$

Note that the coefficients $A_1^{(m)}$ and $A_2^{(m)}$ are related by

$$R_m = \frac{k_1^{(m)}(R_{m+1} - k_2^{(m)}) + k_2^{(m)}(k_1^{(m)} - R_{m+1}) \exp[i \zeta^{(m)}(l_m - l_{m-1})]}{R_{m+1} - k_2^{(m)} + (k_1^{(m)} - R_{m+1}) \exp[i \zeta^{(m)}(l_m - l_{m-1})]} \quad (2)$$

The intensity of the diffuse quanta depends on the intensity of the transmitted wave. Therefore, to calculate the diffuse component, we should have values for the amplitudes of the coherent fields at any point in the multilayer system. This, in turn, can be realized by calculating all the coefficients $A_{1,2}^{(m)}$. Solving the boundary-value problems leads to the following recurrence formula:

$$A_1^{(m)} = A_1^{(m-1)} \frac{(k_1^{(m-1)} - k_2^{(m-1)})(R_m - k_2^{(m)})}{(R_m - k_2^{(m-1)})(k_1^{(m)} - k_2^{(m)})} \times \exp[i l_{m-1}(\zeta_1^{(m-1)} - \zeta_1^{(m)})]. \quad (3)$$

Taking account of the relation between $A_1^{(m)}$ and $A_2^{(m)}$ and using relation (3) in the general solution (1), we obtain all the necessary data for calculating the angular distribution of the intensity diffusely scattered by any layer, say the m th.

The intensity of the diffuse component reflected from the $M - m + 1$ lower layers, I_m^d , recorded at the upper boundary of the m th layer, is found from the differential equation

$$\frac{dI_m^d}{dz} = \frac{\mu^{(m)}}{\gamma_0} I_m^d - 2|\sigma_g^{(m)}|[1 - (E^{(m)})^2] \tau_r^{(m)} I_{0,m}^c,$$

where $I_{0,m}^c = |E_{0,m}^c|^2$ is the coherent intensity of the wave in the direction of transmission; $\mu^{(m)}$ is the normal photoelectric absorption coefficient of the m th layer, and $\tau_r^{(m)}$ is the real part of the correlation length in this layer.

3. EXPERIMENTAL RESULTS

X-ray diffraction studies were carried out on a high-resolution three-crystal diffractometer based on a GUR-8 wide-angle goniometer. The diffraction reflection curves were recorded in a two-crystal dispersion-free scheme and a three-crystal dispersion-free scheme with an asymmetric Ge(001) monochromator. For reflection of (004) CuK_{α_1} radiation, this produced a divergence of the monochromatic radiation of the order of one arcsecond. As the third crystal of the analyzer we used an accurately oriented Ge(001) crystal with (004) reflection. Recording of the three-crystal diffraction reflection curves with ($\vartheta - 2\vartheta$) scanning of the investigated crystal and the crystal-analyzer makes it possible to isolate the coherent component of the diffraction reflection

$$A_2^{(m)} = A_1^{(m)} \left(\frac{k_1^{(m)} - R_{m+1}}{R_{m+1} - k_2^{(m)}} \right) \exp(i \zeta^{(m)} l_m),$$

where l_m is the thickness of the m th layer.

If now by simple mathematical operations we eliminate the coefficients $A_{1,2}^{(m)}$ from consideration and make use of the relation for the amplitude reflection coefficient R_{m+1} , we obtain a simple recurrence formula for the ARC of the entire multilayer crystal

curves with a specified accuracy by substantially decreasing the contribution of the diffuse component. Note that the differential ϑ -curves, recorded with the position of the crystal-analyzer fixed, allow one in a number of cases to uniquely determine the type of structural defect.⁹

We chose AlGaAs/GaAs laser structures with a quantum-sized (10–15 nm) GaAs active region, intended for fabrication of high-power laser diodes, as the objects of study. The structures were grown by the method of metallo-organic gas-phase epitaxy (MOGPE) on accurately oriented GaAs(001) small-dislocation substrates. Such structures can be viewed as model multilayer heterostructures of “interference” type, studies of which make it possible to perfect experimental and theoretical x-ray diffraction methods. In this context, data on crystalline perfection, the deformation profile (concentrational composition), type of defects, and their distribution profile in multilayer heterostructures make it possible to determine the regularities of epitaxial growth and the influence of the type, density, and position of the crystalline defects on such important parameters of high-power laser diodes as the threshold current and degradation time.

With the aim of providing a more detailed description of the procedure of retrieving the parameters of a multilayer system from x-ray diffraction data without unnecessarily extending the length of this paper, we will adduce results of a study of the most characteristic laser heterostructure, 0.2 μm -GaAs (contact layer)/1.3 μm - $\text{Al}_{0.6}\text{Ga}_{0.4}\text{As}$ (emitter)/0.01 μm -GaAs (QW —the active region)/0.445 μm - $\text{Al}_{0.25}\text{Ga}_{0.75}\text{As}$ (waveguide)/1.50 μm - $\text{Al}_{0.4}\text{Ga}_{0.6}\text{As}$ (emitter)/GaAs (buffer layer)/(001) GaAs (substrate). The proposed concentration profile, corresponding to state-of-the-art growth conditions, is depicted in Fig. 1b.

A simple preliminary analysis of the experimental diffraction reflection curves shows that such laser structures possess high crystalline perfection. The epitaxial layers are planar, the interfaces are quite sharp, the density of the defects, their size, and the voltages caused by them are not so large as to lead to smearing of the diffraction patterns. The difference between the experimental diffraction reflection curves and the calculated ones obtained on the assumption of

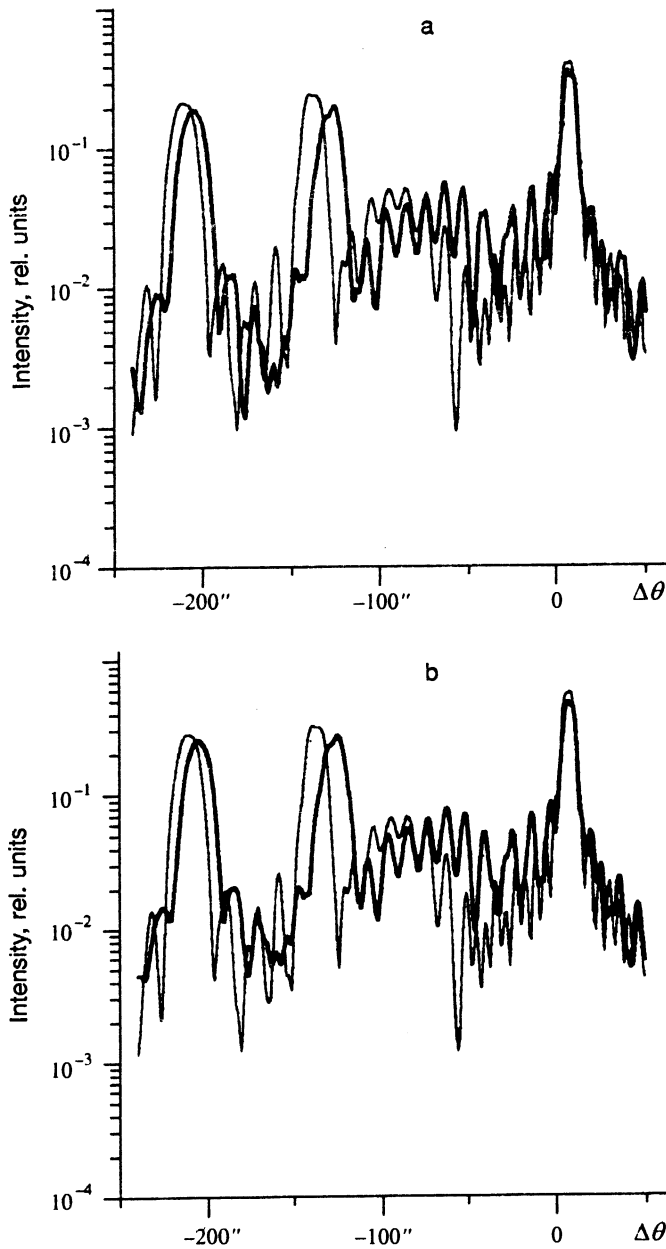


FIG. 2. Experimental and theoretical diffraction reflection curves of a three-crystal (a) and two-crystal (b) diffraction scheme. The theoretical diffraction reflection curves correspond to the concentration profile in Fig. 1b. Here and in the following figures, the heavy solid curve corresponds to the experimental data, and the thin solid curve corresponds to the theoretical.

ideal, defect-free structures suggests that crystalline defects exist in the structures, primarily point defects or small accumulations of point defects (clusters). Subsequent calculational experiments have made it possible to refine the results of the preliminary analysis of the diffraction reflection curves⁸ and to identify those regularities of epitaxial growth which have a substantial effect on the process of defect formation in heterostructures.

4. CALCULATIONAL DIAGNOSIS OF HETEROSTRUCTURES

The parameters of the laser structure (AlGaAs) were found by solving the inverse diffraction problem numerically. This was done by minimizing the error functional

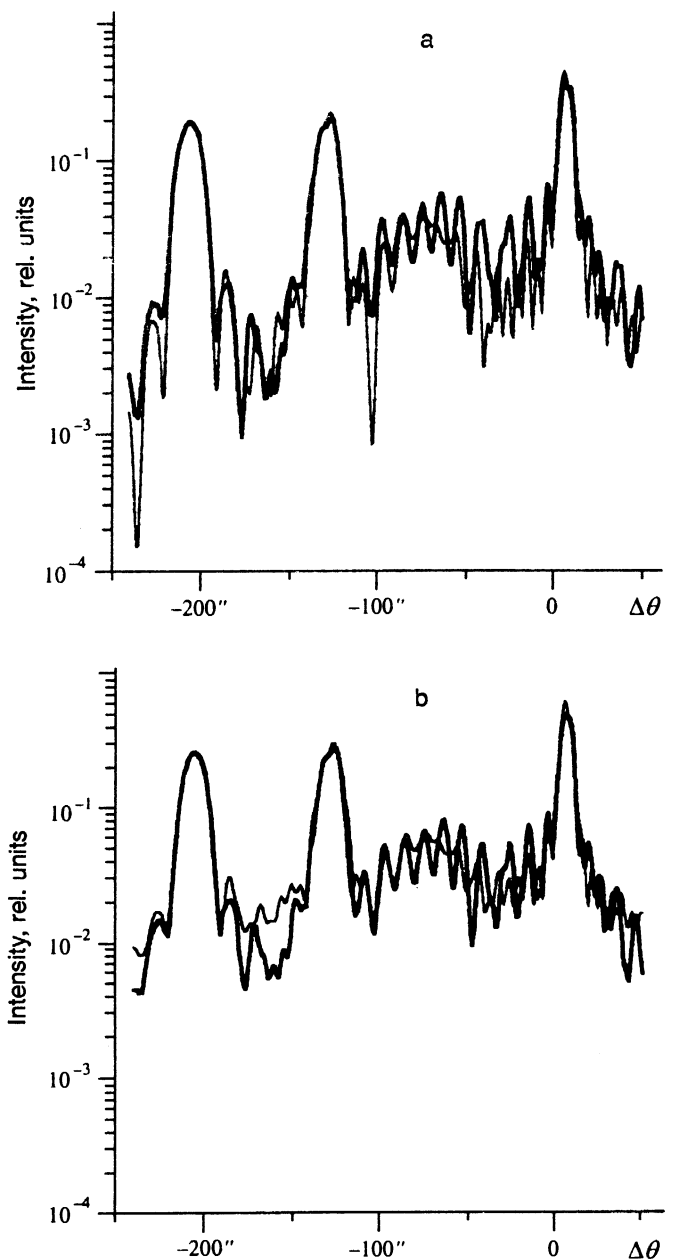


FIG. 3. Three-crystal (a) and two-crystal (b) diffraction reflection curves, corresponding to a five-layer discretization of the concentration profile.

$$R = \sum_{i=1}^k (R_i^e - R_i^t)^2 + \sum_{i=1}^k (R_{i,c}^e - R_{i,c}^t)^2 = R(\mathbf{X}, \mathbf{E}, \mathbf{r}), \quad (4)$$

where $R_i^{e,t}$ are the reflection coefficients [experimental and theoretical] in the two-crystal scheme, $R_{i,c}^{e,t}$ are the corresponding reflection coefficients in the three-crystal ($\vartheta-2\vartheta$) scanning scheme, and k is the number of experimental points, \mathbf{X} , \mathbf{E} , and \mathbf{r} are $(M+1)$ -dimensional vectors which define the deformation profile of the heterostructure, the value of the static Debye-Waller factor, and the average size of the defects in each layer. For the calculated characteristics of the multilayer structure to adequately reflect its actual structure, it is necessary to take into account all parameters noticeably influencing the formation of the experimental

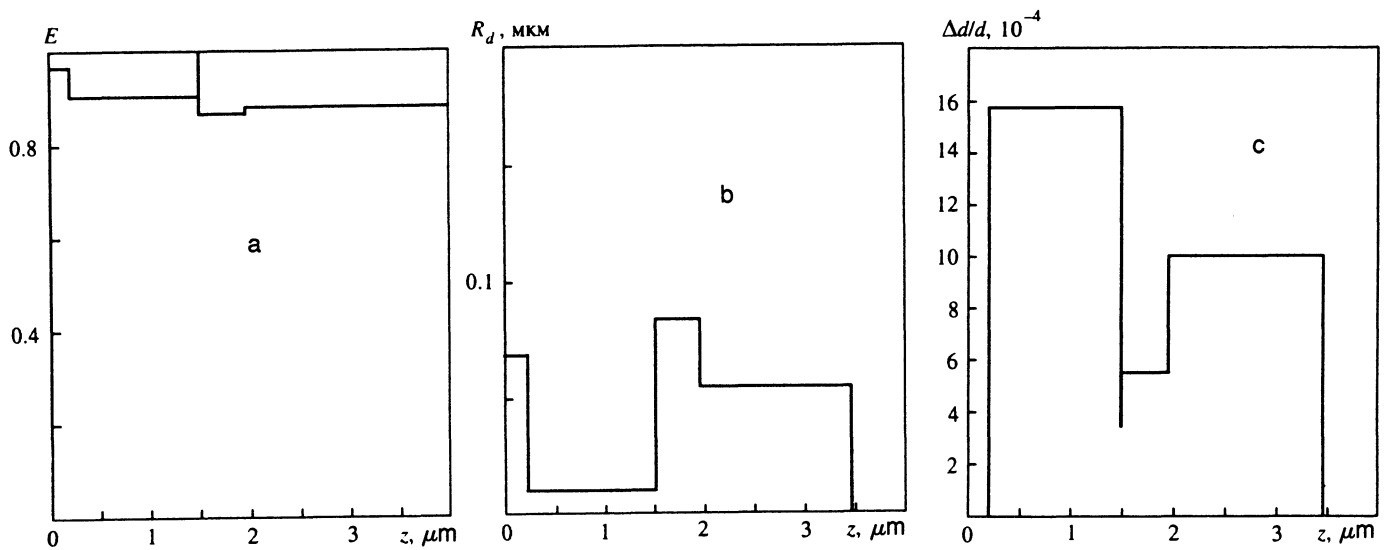


FIG. 4. Distribution of the static Debye–Waller factor (a), defect radius (b), and deformation profile (c) with depth into the laser heterostructure for the five-layer discretization model. The theoretical curves, corresponding to these distributions of the heterostructure parameters, are shown in Fig. 3.

x-ray diffraction spectrum, in particular, the divergence of the rays emitted by the Roentgen tube and incident on the reflecting crystals of the corresponding diffraction scheme (the monochromator, the sample, and, in the case of three-crystal diffractometry, the analyzer).²⁴

The minimization of functionals of the form (4) is associated with significant calculational difficulties due to the multiplicity of local minima, the large number of parameters, and the nonlinearity of the functional. The application of gradient methods is hampered by the complexity of calculations of such functionals. In the present paper, we have used the direct search method (the simplex method) in the presence of constraints imposed on the unknown vectors \mathbf{X} , \mathbf{E} , and \mathbf{r} .²⁰ As our starting approximation, we chose a concentration profile corresponding to a design draft of the given heterostructure (Fig. 1b). The difference between the experimental diffraction spectrum and the theoretical reflection curve can be seen in Fig. 2. Here and in the following figures the heavy solid line represents the experimental reflection curves and the thin solid line, the theoretical reflection curves. In the solution of the inverse diffraction problem based on this five-layer model of the laser structure, satisfactory minimization was not achieved (Fig. 3). Figure 4 shows the parameters of the structure obtained by this minimization. Note that at this step we have held to the following rules: first, Vegard's law is fulfilled for all the AlGaAs compositions; second, the magnitude of the tetragonal deformation corresponds to the elastic strains of the mated materials without account of relaxation processes. In the real situation, obviously, relaxation processes with formation of defects are unavoidable. They lead in one way or another to changes in the deformation profile. Apparently, these processes should manifest themselves more noticeably in the region of the heterotransitions when the conditions of epitaxial growth change. Therefore additional calculations were carried out for the given system with division into a larger number of layers. Taking account of the behavior of the concentration

profile of the heterostructure (compositional makeup, number of heteroboundaries, thicknesses of the layers), this number was set to 23. As our initial approximation of the calculational diagnosis we used the original five-layer model of the laser structure. Figure 5 displays the experimental diffraction reflection curves and the calculated curves corresponding to the 23-layer system. The calculated distributions of the structural characteristics with depth into the heterostructure, such as the profile of the elastic deformations, the distribution of the static Debye–Waller factor, and the distribution of the mean radius of the defects are shown in Fig. 6.

For our preliminary calculations we used an artificial constructed Gaussian correlation function

$$g(\xi) = \exp(-\pi\xi^2/4\tau_0^2), \quad (5)$$

where τ_0 is the most general characteristic of the medium and has the sense of Kato's correlation length.²⁵ The correlation length allows one to estimate the mean size of the defects.⁴ At the intermediate step of the solution it became clear that the correlation length τ_0 within each separate layer of the heterostructure (excluding the region of the heteroboundaries) is a constant quantity of order $0.01 \mu\text{m}$. Therefore these are most likely imperfections caused by the point defects or clusters of them. Such defects are well described by a "Coulomb" defect model with random displacements²⁶

$$\mathbf{u}(\mathbf{r}) = \begin{cases} A\mathbf{r}/r^3, & \text{if } |\mathbf{r}| > R_d, \\ \text{random value} & \text{if } |\mathbf{r}| \leq R_d, \end{cases} \quad (6)$$

where R_d is the radius of the randomly distributed isotropic inclusion. The quantity A is defined as the power of the defect.²³ For the given model the correlation function has the form

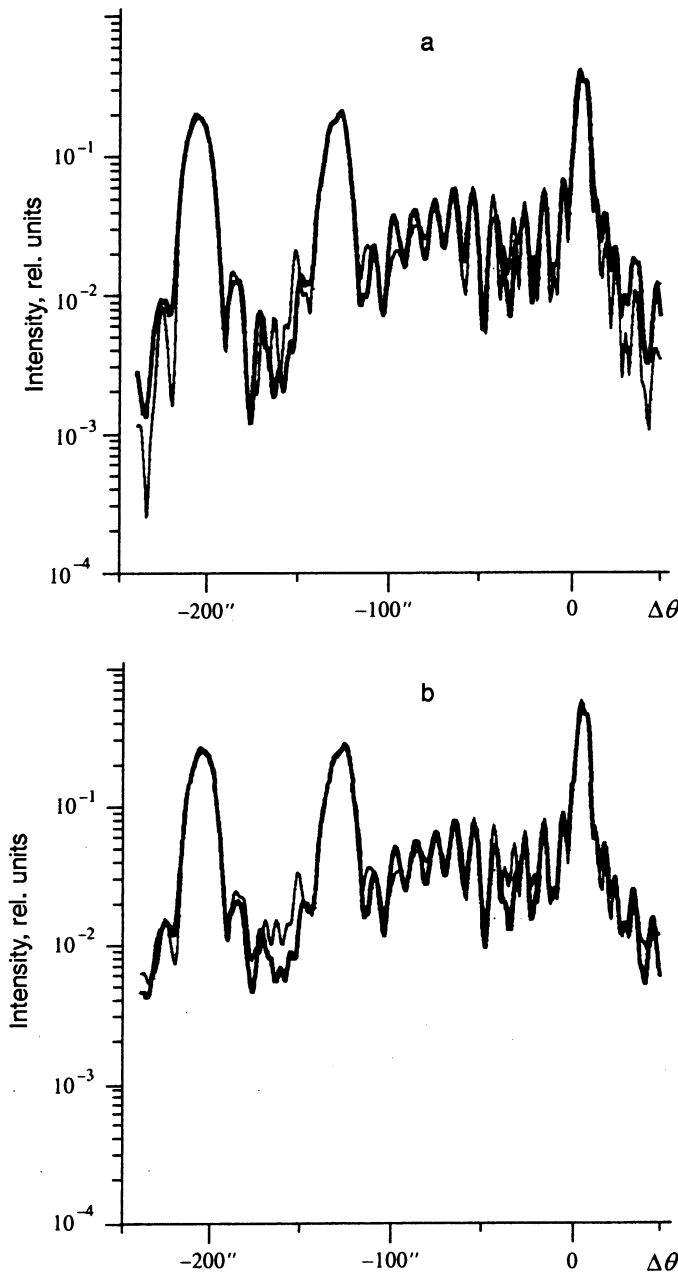


FIG. 5. Three-crystal (a) and two-crystal (b) diffraction reflection curves corresponding to 23-layer discretization of the concentration profile.

$$g(\rho) \approx \frac{1}{V_{cl}(1+\tilde{A}^2)} \left\{ V_{cl} \left(1 - \frac{3\rho}{4R_d} + \frac{\rho^3}{16R_d^3} \right) + 2A^2 |g|^2 \right. \\ \left. \times \left[\frac{-\pi\rho(\cos\eta+1)}{8R_d^2} + \frac{2\pi}{3R_d} \right] \right\} \quad \text{for } \rho \leq 2R_d, \quad (7)$$

$$g(\rho) \approx \frac{1}{V_{cl}(1+\tilde{A}^2)} \left\{ 2A^2 |g|^2 \left[\frac{\pi \sin^2 \eta}{\rho} + \frac{2\pi(3\cos^2 \eta - 1)R_d^2}{3\rho^3} \right] \right\}, \quad \text{for } \rho > 2R_d.$$

Here the angle η is the angle between \mathbf{g} and ρ , $V_{cl} = 4\pi R_d^3/3$ is the volume of the defect, and $\tilde{A} = A|g|/R_d^2$. Since the cal-

ulation of correlation functions introduced as one of the main parameters of a statistical, dynamical theory of diffraction^{11-15,23,25} is a separate problem unto itself, the procedure and analysis of these calculations for various models of microdefects are not laid out here. Figure 7 presents profiles of correlation functions (5) and (7) for various powers [Eq. (7)] and sizes of the defects (correlation lengths τ_0).

5. DISCUSSION OF RESULTS

It is well known that the formation of structural defects in heterostructures during epitaxial growth (assuming ideal pregrowth preparation of the substrates) is due to relaxation of the elastic strains, the magnitude of which is determined by the mismatch of the lattice parameters of the epitaxial structure at the growth temperature. The larger this value, the greater the elastic strains in the growing structure and, consequently, the smaller the value of the critical thickness of the epitaxial layer at which, for all other growth conditions optimal, relaxation of the elastic strains will begin. Obviously, the probability of growth defect formation is higher when growing epitaxial layers of greater thickness and with greater mismatch of the lattice parameters for a given epitaxial growth temperature. It is especially important to take this fact into account when investigating laser heterostructures with quantum-sized active regions.

Most critical for the presence of defects are the active region and the waveguide segments immediately adjacent to it. The appearance in this region of uniformly distributed point defects, formed at the initial stage of relaxation of the elastic strains, has a direct effect on the degradation characteristics of laser diodes since it is in the optical lasing regime under conditions of high electron-hole plasma density and high optical radiation density that structural transformation of the growth defects begins. This process resembles the defect formation process during epitaxial growth. The defects grow, clusters of point defects form in the region of maximum current density and optical radiation density, and then small dislocations (dislocation loops) form, which give rise to defects of "dark lines and spots" in the active region and, as a result, a rapid drop in the quantum yield of the laser diode. The higher the initial density of crystalline defects in the laser structure, the faster will be the process of their structural transformation "under loading" and, stimulated by the process, the degradation of the electrophysical parameters. It may be supposed that the process of structural transformation of growth defects in laser diodes takes place with "positive" feedback—the higher the initial defect density, the higher the threshold current and the higher the operating temperature of the active region and the waveguides, and, consequently, the higher the rate of transformation of the growth defects and degradation of the laser diode. Apparently, this may be the explanation for the catastrophic degradation of laser diodes fabricated from structures with low crystalline perfection. Any local heat losses, for example, to mirrors, should also increase the rate of degradational transformations of defects.

The results of our study show that the highest defect concentration is concentrated in the region of the heter-

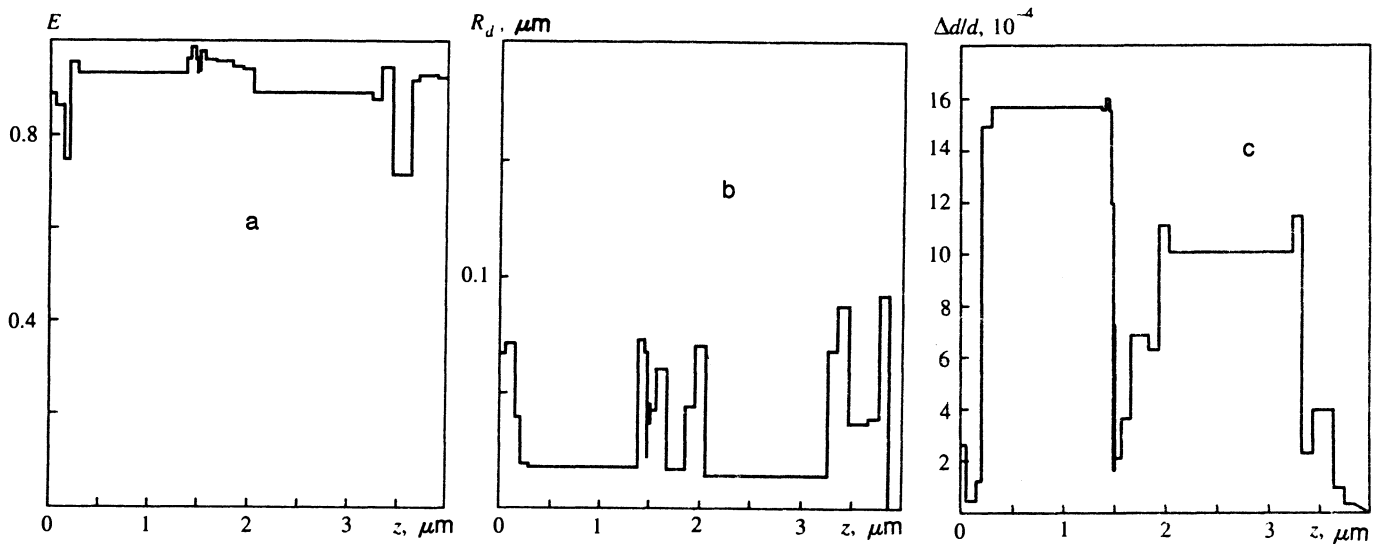


FIG. 6. Distribution of the static Debye-Waller factor (a), defect radius (b), and deformation profile (c) vs thickness of the laser heterostructure for the 23-layer discretization model. The theoretical curves corresponding to these distributions of the heterostructure parameters are shown in Fig. 5.

boundaries: the buffer layer-epitaxial layer $\text{Al}_{0.4}\text{Ga}_{0.6}\text{As}$ (first emitter) and epitaxial layer $\text{Al}_{0.6}\text{Ga}_{0.4}\text{As}$ (upper emitter)-contact layer of GaAs. Inside the volume of the thick emitter layers of the heterostructures $\text{Al}_{0.6}\text{Ga}_{0.4}\text{As}$ and $\text{Al}_{0.4}\text{Ga}_{0.6}\text{As}$ the defect concentration is approximately the same (of order $3 \cdot 10^{15} \text{ cm}^{-3}$ and $14 \cdot 10^{15} \text{ cm}^{-3}$, respectively). The average diameters of the defects are also close and are equal to 17 nm in the $\text{Al}_{0.6}\text{Ga}_{0.4}\text{As}$ layer and 12 nm in the $\text{Al}_{0.4}\text{Ga}_{0.6}\text{As}$ layer. These defects are a particular type of point defects and their clusters. At the heteroboundaries the defects are larger (≈ 0.05 – $0.1 \mu\text{m}$). The structural defects are strong in the region of the heteroboundary of the substrate (buffer layer)-heterostructure, apparently because the substrate surface is insufficiently pure. Defects, presumably oxygen clusters, are formed at the growth surface of the substrate at the initial stage of the gas epitaxy process (during heating from room temperature to the temperature of epitaxial growth) as a consequence of insufficient purification of the hydrogen. An increase in the degree of amorphization (decrease in the value of the static factor) with simultaneous

increase of the defect dimensions in the near-surface region of the heterostructure is due to relaxation of the elastic strains and migration of the defects to the upper boundary during growth. The second reason for the appearance of defects at the emitter-contact layer boundary may be stopping the growth process and putting hydrogen through the reactor to obtain a sharp interface (in composition and bonding impurity). In the quantum-sized active region the static Debye-Waller factor is close to unity, which indicates a low defect concentration; however, the elastic strains are quite large. It is interesting to note that the dimensions of the defects in this region are close to the dimensions of the defects in the volume of the thick layers. This most probably indicates the presence of point defects.

We should also point out that the GaAs substrate in the investigated heterostructure was not “absolutely ideal.” Our calculations demonstrate the presence of a low defect concentration in the volume of the substrate. The static Debye-Waller factor of the substrate was 0.96.

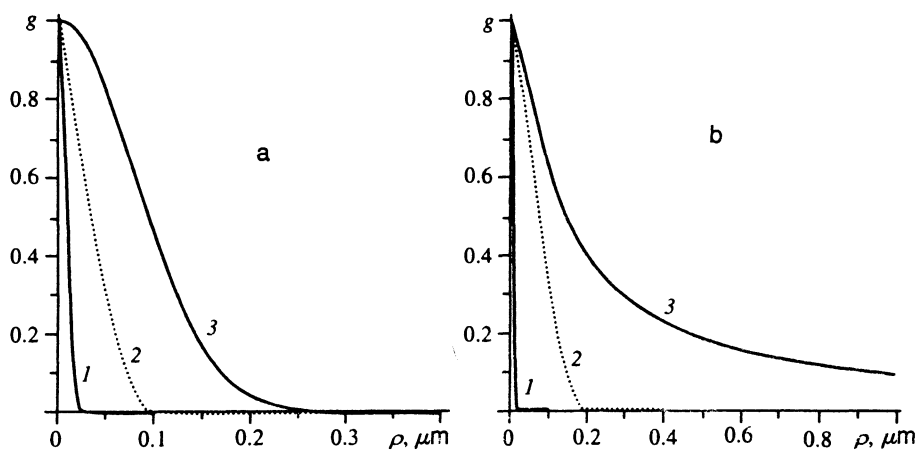


FIG. 7. Correlation functions of “Gaussian” type (a) and of “Coulomb” type (b) for various sizes and powers of the defects: a) correlation length τ_0 : 1—0.01 μm , 2—0.05 μm , 3—0.1 μm ; b) defect radius R_d (defect power A): 1—0.01 μm (10^{-7}), 2—0.05 μm (10^{-7}), 3—0.1 μm (10^{-3}).

6. CONCLUSION

The determination of the structural perfection of homo- and hetero-epitaxial structures is one of the most important problems of high-resolution x-ray diffractometry in growth (epitaxial) technology. This problem cannot be considered as a narrow, applied problem since the results obtained indicate the existence of fundamental regularities in the processes of epitaxial growth and defect formation, and also a close interrelationship between the conditions of epitaxial growth and the crystalline perfection of the epitaxial layers and the heterostructures as whole. The very concept of crystalline perfection of heterostructures should include perfection of the substrate and the epitaxial layers, planarity of the epitaxial layers, and sharpness of the interfaces, the profile of the distribution of strains in the structure, the presence of defects, a classification of their types, and the profile of the distribution of the latter in the multilayer structure as a whole.

The method proposed in this paper for obtaining information about the structural characteristics of a multilayer system, using high-resolution x-ray diffraction data, could use further refinement. In particular, we did not succeed in achieving "absolute" agreement between the theoretical and experimental diffraction reflection curves, since we did not vary the thicknesses of the discretization layers of each structure. Taking this factor into account would, of course, not result in any fundamental differences in the calculation of the parameters of the heterostructure, but would allow a more accurate determination of the spatial distribution of the deformations and defects. On the other hand, this would complicate an already complicated problem of computational diagnostics.

Despite the laboriousness of the process of determining the characteristics of laser structures, the fruitfulness of the present approach is obvious. The next step in the implementation of the method will be the solution of the inverse problem of diffraction in gradient structures and superlattices. It would also be interesting to compare the results obtained with the present method and with other methods.^{18,19,21,27}

The authors are grateful to V. A. Bushuev for discussion of the results. The work was carried out with the financial support of the International Scientific Fund, (Grant No. NU6000).

*A. F. Ioffe Physicotechnical Institute, Russian Academy of Sciences, St. Petersburg.

- ¹A. M. Afanas'ev, P. A. Aleksandrov, R. M. Imamov, *X-ray Diffraction Diagnostics of Submicron Layers* [in Russian], Nauka, Moscow (1989).
- ²A. M. Afanas'ev and V. G. Kon, *Zh. Éksp. Teor. Fiz.* **74**, 300 (1978) [Sov. Phys. JETP **47**, 154 (1978)].
- ³M. A. Andreeva, S. M. Ikraev, and V. G. Semënov, *Zh. Éksp. Teor. Fiz.* **105**, 1767 (1994) [JETP **78**, 956 (1994)].
- ⁴S. N. Voronkov, D. I. Piskunov, F. N. Chukhovskii, and S. K. Maksimov, *Zh. Éksp. Teor. Fiz.* **92**, 1099 (1987) [Sov. Phys. JETP **65**, 624 (1987)].
- ⁵A. de Visser, V. I. Kadushkin, V. A. Kul'bachinskii *et al.*, *Zh. Éksp. Teor. Fiz.* **105**, 1701 (1994) [JETP **78**, 918 (1994)].
- ⁶X. Chu and B. K. Tanner, *Semicond. Sci. Technol.* **2**, 765 (1987).
- ⁷L. Tapfer and K. Ploog, *Phys. Rev. B* **40**, 9802 (1989).
- ⁸N. N. Faleev, L. I. Flaks, S. G. Konnikov *et al.*, *Phys. Stat. Sol. (a)* **120**, 327 (1990).
- ⁹T. A. Argunova, R. N. Kyutt, S. S. Ruvimov, and M. P. Scheglov, *Inst. Phys. Conf. Ser. No. 117*, Section 9, 669 (1991).
- ¹⁰P. F. Fewster, *Appl. Surf. Sci.* **50**, 9 (1991).
- ¹¹V. A. Bushuev, *Fiz. Tverd. Tela* **31**, 70 (1989) [Sov. Phys. Solid State **31**, 1877 (1989)].
- ¹²V. I. Punegov, *Kristallografiya* **35**, 576 (1990) [Sov. Phys. Crystallography **35**, 336 (1990)].
- ¹³V. I. Punegov, *Fiz. Tverd. Tela* **33**, 234 (1991) [Sov. Phys. Solid State **33**, 136 (1989)].
- ¹⁴V. I. Punegov, *Phys. Stat. Sol. (a)* **136**, 9 (1993).
- ¹⁵V. I. Punegov, *Pis'ma Zh. Tekh. Fiz.* **20**(2), 25 (1994) [Tech. Phys. Lett. **20**, xxx (1994)].
- ¹⁶V. S. Speriosu, M.-A. Nicolet, J. L. Tandon, and Y. C. M. Yeh, *J. Appl. Phys.* **57**, 1377 (1985).
- ¹⁷C. R. Wie, J. C. Chen, H. M. Kim *et al.*, *Appl. Phys. Lett.* **55**, 1774 (1989).
- ¹⁸A. V. Goncharskii, A. V. Kolpakov, and A. A. Stepanov, *Inverse Problems of X-ray Diffractometry* [in Russian], Latvian University, Riga (1992).
- ¹⁹S. P. Darbinyan, P. V. Petrashen', and F. N. Chukhovskii, *Pis'ma Zh. Éksp. Teor. Fiz.* **37**, 854 (1992).
- ²⁰D. Himmelblau, *Applied Nonlinear Programming* [McGraw-Hill, New York (1972)].
- ²¹A. M. Afanas'ev and S. S. Fanchenko, *Dokl. Akad. Nauk SSSR* **287**, 1395 (1986) [Sov. Phys. Dokl. **31**, 280 (1986)].
- ²²V. K. Ignatovich, *Zh. Éksp. Teor. Fiz.* **97**, 1616 (1990) [Sov. Phys. JETP **70**, 913 (1990)].
- ²³M. A. Krivoglaz, *Theory of X-Ray and Thermal Neutron Scattering by Real Crystals* [Plenum, New York, (1969)].
- ²⁴Z. G. Pinsker, *X-Ray Crystalline Optics* [in Russian], Nauka, Moscow (1982).
- ²⁵N. Kato, *Acta Cryst. A* **36**, 763, 770 (1980).
- ²⁶V. Holy, *Acta Cryst. A* **40**, 675 (1984).
- ²⁷S. G. Podorov, V. I. Punegov, and V. A. Kusikov, *Fiz. Tverd. Tela* **36**, 827 (1994) [Solid State Phys. **36**, 454 (1994)].

Translated by Paul F. Schippnick